Bulletin of the Seismological Society of America, Vol. 86, No. 5, pp. 1314–1330, October 1996

Determination of Local Magnitude Using BDSN Broadband Records

by Robert A. Uhrhammer, Suzanna J. Loper, and Barbara Romanowicz

Abstract The Berkeley Seismographic Station operated standard Wood–Anderson torsion seismographs from 8 April 1928 through 16 January 1994. These seismographs are historically significant in that their seismograms have been used to determine local (Richter) magnitude of earthquakes that occurred in northern and central California and adjacent regions, routinely since 1948 and *ad hoc* back to 1928. Broadband digitally recording seismographs were co-sited at four stations with Wood–Anderson instruments to compare the records. The Wood–Anderson seismographs became redundant for the purpose of determining the maximum horizontal trace amplitudes once procedures were developed to synthesize their seismograms accurately from the broadband digital recordings. Operation of the Wood–Anderson seismographs was subsequently discontinued. This article demonstrates the ability to determine an unbiased measure of local magnitude from synthesized Wood–Anderson seismograms, thereby maintaining a seamless catalog of local magnitude at Berkeley.

Introduction

The local magnitude (hereafter denoted M_L) for earthquakes, occurring in northern and central California and adjacent regions, has been routinely determined by Berkeley and reported in the *Bulletin of the Seismographic Stations of the University of California* since 1948 (Romney and Meeker, 1949). The main use of the M_L scale has been to provide a simple and quantitative measure of the relative size of earthquakes. M_L is determined from the "maximum trace amplitude" recorded photographically by "standard 0.8-sec-period Wood–Anderson torsion seismographs" (hereafter denoted WA) (Richter, 1935; Gutenberg and Richter, 1942; Richter, 1958).

As shown by Uhrhammer and Collins (1990), synthesized Wood–Anderson (hereafter denoted SWA) seismograms can be routinely generated from horizontal-component broadband digital records (with sampling rates of 20 samples/sec or higher), for the purpose of determining the maximum trace amplitude. When generating SWA records, it is crucial to note that the response of WA seismographs of the type operated in the UC Berkeley station network is $V_S = 2080$, $T_S = 0.8$ sec, and $h_S = 0.7$ critical (Uhrhammer and Collins, 1990) and not $V_S = 2800$, $T_S = 0.8$ sec, and $h_S = 0.8$ as has been commonly assumed and reported repeatedly in the seismological literature since the original article of Anderson and Wood (1925).

The goal of this study is to verify the successful generation of SWA seismograms through comparison of maximum amplitudes and waveforms and subsequently determine station magnitude adjustments (hereafter denoted δM_L) for the determination of M_L using the recently upgraded broadband instrumentation in the Berkeley Digital Seismic Network (BDSN) in northern and central California (Romanowicz *et al.*, 1992). The overall aim is to be able to continue the reporting of M_L, as has been done routinely since 1949 and *ad hoc* for events of interest dating back to 1927, without introducing a significant bias into the Berkeley earthquake catalog.

Historical Perspective

WA seismographs operated continuously longer than any other instrument to date in the Berkeley seismographic network. WA seismographs began operating at Lick Observatory on top of Mt. Hamilton (MHC) on 8 April 1928 (Uhrhammer, 1989), and they operated continuously until 16 January 1993. Dates of operation of the five Berkeley stations housing WA seismographs and of the BDSN broadband stations used in this study are presented in Table 1.

WA seismographs became particularly important after Richter (1935) introduced the concept of an instrumental earthquake magnitude scale in which the "local magnitude (M_L)" is determined from

$$M_L = \log A - \log A_0(\Delta) + \delta M_L, \qquad (1)$$

where A is the maximum trace amplitude recorded on a WA seismogram, $A_0(\Delta)$ is a distance (Δ)-dependent attenuation function, and δM_L is a station-dependent M_L adjustment. A detailed history and development of the M_L scale is presented by Boore (1989). Routine reporting of M_L in the *Bul-*

Table 1
BDSN Station Information

Stn	Lat	Lon	Elev (m)	Inst	Dates* of Operation	Site	Lithology†	μ‡	κ§
ARC	40.877	−124.075	60.0	WA	06/20/52–01/15/93	Ground floor	Sandstone	1.4	−0.2
				STS-2	05/28/92–current				
								1.1¶	
BKS	37.877	−122.235	276.0	WA	07/01/62–01/16/93	Mining drift	Shale	(2.6)	−1.3
				STS-1	05/11/87–current				
BRK	37.873	−122.260	81.0	WA	01/01/34–05/31/62	Basement pier	Franciscan	27	0.0
				STS-2	02/01/94–current				
CMB	38.035	−120.385	719.0	STS-1	07/01/86–current	Surface vault	Limestone	3.1	0.0
HOPS	38.994	−123.072	299.1	STS-1	03/01/95–current	Buried vault	Franciscan	2.7	+0.3
JRSC	37.404	−122.238	103.0	STS-2	06/30/94–current	Surface vault	Serpentine	1.2	−0.3
KCC	37.324	−119.318	914.3	STS-1	12/08/95–current	Tunnel	Granite	3.4	0.0
MHC	37.342	−121.642	1282.0	WA	04/08/28–01/16/93	Ground floor	Graywacke	1.4‖	+1.1
				STS-1	09/10/86–current			(3.0)	
MIN	40.345	−121.605	1495.0	WA	01/02/39–01/15/94	Surface vault	Tuff	0.7	0.0
				STS-1	03/19/93–current				
ORV	39.556	−121.500	360.0	STS-1	07/24/93–current	Surface vault	Basalt	3.5	0.0
PKD1	35.889	−120.425	5.0	STS-2	10/22/91–current	Concrete slab	Quaternary	0.7	−1.2
SAO	36.765	−121.445	350.0	STS-1	01/28/88–current	Buried vault	Granite	2.8	−0.6
STAN	37.404	−122.174	158.0	STS-2	04/01/91–06/30/94	Building slab	Alluvium	0.3	+0.1
WDC	40.580	−122.540	300.0	STS-2	07/14/92–current	Mining drift	Gneiss	4.5	−0.5
YBH	41.732	−122.711	1100.0	STS-1	07/24/93–current	Mining drift	Metavolcanic	4.6	−1.0

*Dates of operation of WA and digitally recorded BDSN instruments.
†Bedrock lithology.
‡Estimated site rigidity in units of 10^{11} dynes/cm^2.
§Estimated terrain curvature in km^{-1}.
¶μ for dominant subsurface Orinda formation underlying BKS (David L. Jones, personal comm. 1995).
‖μ for dominant subsurface Franciscan sandstones underlying MHC (David L. Jones, personal comm. 1995).

letin of the Seismographic Stations began in 1948 (Romney and Meeker, 1949). M_L for earthquakes occurring prior to 1948 was estimated on an *ad hoc* basis and tabulated in Bolt and Miller (1975). M_L was determined to 0.1 resolution back to 1942 and to 0.5 resolution prior to 1942. Only a few events have an assigned M_L prior to March 1934.

M_L was routinely calculated by using the Nordquist nomograph (Gutenberg and Richter, 1942) prior to the advent of personal computers (PC's) in the Seismographic Station. The historical δM_L shown in Table 2 was used when calculating M_L. When PC's were installed, in 1984, an algorithm was developed and used for the calculation of M_L. When the digitally recorded BDSN broadband instrumentation came on-line in 1986 (Bolt *et al.*, 1988), algorithms were developed and used for calculation of M_L from the maximum trace amplitudes registered on SWA seismograms.

Table 2
BDSN δM_L

Station	δM_L (Historical)	δM_L (this study)
ARC	+0.2*	+0.209 ± 0.028
BRK	+0.2†	+0.198 ± 0.033
BKS	0.0*	−0.035 ± 0.017
MHC	+0.1†	+0.128 ± 0.018
MIN	−0.1*	−0.107 ± 0.026

*Tocher (personal comm., 1979)
†Gutenberg and Richter (1942).

Methodology

The primary goal is to maintain continuity in the determination of M_L as the metrology has evolved from analog to digital instrumentation. A related goal is to maintain the simplicity of Richter's original methodology for determining M_L as given in equation (1) and described in his 1935 article. The analysis consists of four steps designed with the aim of verifying that a seamless continuity in the determination of M_L can be maintained when converting from measuring the maximum trace amplitudes on WA seismograms to measuring them on SWA seismograms. First, we verify the historical δM_L that was used in the routine determination of M_L from the WA seismograms using events in Fig. 1. Then, we describe how the SWA seismograms are routinely generated for the purpose of measuring the maximum trace amplitudes. Next, we compare WA seismograms with the corresponding SWA seismograms, at the four sites that housed both WA seismographs and broadband seismographs, and determine δM_L's for use with the SWA seismograms. Finally, we determine δM_L's for use with the rest of the BDSN broadband stations using events in Fig. 2.

When calculating δM_L's for the BDSN stations, we discovered that there were systematic variations in the M_L residual distribution with both distance and azimuth. However, in keeping with the original methodology of Richter (1935), we solve only for perturbations to the attenuation function $[-\log A_0(\Delta)]$.

Verification of the Historical δM_L's

To verify the historical δM_L's (Table 2) used in the routine determination of M_L from WA seismograms, we proceed in two steps: first, determine simultaneously the δM_L's for ARC, BKS, MHC, and MIN; then, solve for the δM_L for BRK by comparison with BKS. In the simultaneous least-squares inversion for the δM_L's at ARC, BKS, MHC, and MIN, we require that every event used in the inversion be recorded on-scale by all eight WA's (two components at each station) with an amplitude of at least 0.3 mm, and we impose the constraint that the sum of the δM_L's is stationary. This guarantees that the M_L's for each event will be identical, hence unbiased, when using either the historical δM_L's or the least-squares–derived δM_L's. The δM_L for BRK is solved for separately by comparison with BKS because WA's have not been operated at BRK since BKS was opened in 1962.

Between 1984 and 1992, 71 earthquakes, listed in Appendix A and plotted in Figure 1, that occurred in central and northern California and vicinity were recorded by the WA's at ARC, BKS, MHC, and MIN and met the above criteria. The stationarity constraint requires that the sum of the least-squares–derived δM_L's is $+0.2$, the same as the sum of the historical δM_L's at the ARC, BKS, MHC, and MIN. The results are given in Table 2. Note that the least-squares–derived δM_L's are the same as the historical δM_L's when rounded to the nearest tenth. Thus we have verified the historical δM_L's for these four stations.

A BDSN broadband seismograph was installed temporarily at BRK, on the original WA pier in Haviland Hall on the Berkeley campus, in order to record some events for comparison with BKS. The WA at BKS was already discontinued, so we compared the corresponding SWA seismograms at BRK and BKS for five regional earthquakes, and the inferred δM_L for BRK is given in Table 2. Note that the SWA-derived δM_L is not significantly different than the historical δM_L. Thus we have also verified the historical δM_L for BRK.

Generation of SWA Seismograms

SWA seismograms are routinely generated, for the purpose of measuring the maximum trace amplitudes, using frequency domain convolution. The response of WA seismographs is described in detail by Uhrhammer and Collins (1990), and calibration parameters for the individual WA seismographs in the Berkeley network are given in Appendix B. We adopt the complex pole pair:

$$s(\omega) = V_S \cdot [\omega_S h_S \pm i\,\omega_S (1 - h_S^2)^{1/2}], \qquad (2)$$

where $V_S = 2080$, $h_S = 0.7$, $\omega_S = 2\pi/T_S$, and $T_S = 0.8$ sec as the representative displacement frequency response of a WA seismograph, for use in calculating SWA seismograms. This is essentially equivalent to a two-pole high-pass But-

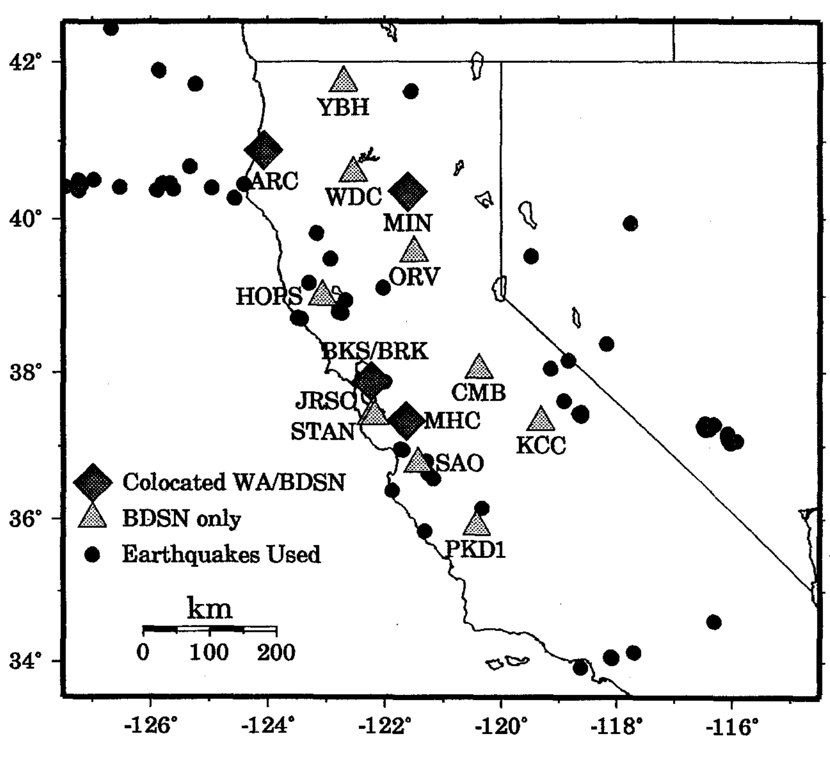

Figure 1. Map of California and vicinity showing the locations of the co-sited WA and BDSN broadband stations (diamonds), the rest of the BDSN stations (triangles), and the earthquakes (solid circles) used to verify the historical δM_L.

terworth filter with a 1.25-Hz corner frequency and a gain of 2080.

The routine procedure is to generate the SWA seismogram, by deconvolving the BDSN broadband signal to ground displacement and convolving the WA response (equation 2), and then to select the largest discrete sample amplitude for the "maximum trace amplitude" described by Richter (1935). We use the 80 samples/sec broadband channels (HHN and HHE), which have a 32-Hz bandwidth, for generating the SWA seismograms in order to minimize the discrete sampling error. It should be noted that we do not routinely remove the finite impulse response (FIR) antialias filter in the deconvolution process, which results in a small-frequency-dependent error, which is discussed in the next section. The 20 samples/sec broadband channels (BHN and BHE), which have an 8-Hz bandwidth, can also be used with the proviso that the "maximum trace amplitude" could be significantly underestimated.

Comparison of SWA and WA Seismograms

BDSN broadband Streckeisen seismographs with 24-bit resolution Quanterra data loggers were co-sited at the four stations housing WA seismographs (ARC, BKS, MHC, and MIN) in order to compare the WA and SWA seismograms for local and regional events. Maximum trace amplitudes recorded on WA seismograms were measured using a 0.1-mm resolution comparator, measuring from the "zero" line of the trace to the midpoint of the trace at the maximum peak. Corresponding SWA records were generated from the co-sited BDSN records using the convolution procedure described in the previous section. Calculation of M_L using SWA seismograms requires that the "maximum trace amplitude," but not necessarily the high-frequency detail, be accurately reproduced. Maximum trace amplitudes measured on numerous WA and corresponding SWA seismograms were compared, and a representative sample is given in Appendix C. From this comparison, we determined that the difference between the WA and SWA measured maximum trace amplitudes was not significant. This implies that the δM_L given in Table 2 is also appropriate for determining M_L from the SWA seismograms. The WA δM_L in Table 2 was thus adopted for determining M_L when using the SWA records.

Due to space limitations, a single WA seismogram was selected as representative for detailed analysis here. The selected ARC E–W component WA seismogram and the corresponding SWA seismogram are shown in Figure 3. Visual differences can immediately be seen between the two seismograms, particularly at the higher frequencies present in the coda. Note, however, that the maximum trace amplitudes registered by the two seismograms differ by less than 2%. This is fairly typical and representative of the differences between the WA and SWA seismograms we have compared. The implication is that we can reliably generate a SWA seismogram for the purpose of measuring the maximum trace amplitude.

A more detailed examination of the characteristics of the SWA seismogram is given in Figure 4. Note that the dominant frequency band associated with the maximum trace amplitude is approximately 4.5 to 6 Hz. At these frequencies, there are two competing error sources that act to bias the measured maximum trace amplitude. The first source is due to ignoring the FIR antialias filter (mentioned in the previous section), and the second source is due to the discrete sampling. The net result is that the log of the maximum trace amplitude, and hence the M_L estimate, can be in error by as much as ± 0.015 when the dominant frequencies are below ~7.5 Hz. Above ~7.5 Hz, the amplitudes will always be biased low, which also explains the observed differences between the WA and SWA high-frequency codas. It is fortuitous that the two error sources tend to cancel each other out at the dominant frequencies (<7.5 Hz) associated with the maximum trace amplitudes.

Visual comparisons between SWA and WA seismograms were encouraging, and we were interested in making a more quantitative study of the waveforms via coherency analysis. In order to make such a comparison, we scanned and digitized a number of WA seismograms recorded at ARC, BKS, MHC, and MIN. However, our results told us more about how well the WA records can be scanned and digitized than how well SWA replicate WA records. Two basic limitations were encountered, the physical resolution of the scanner and the high-frequency trace-following characteristics of the digitizer, which precluded digitization of the original WA seismograms with sufficient accuracy to be useful for coherency analysis. The scanner has a resolution of 400 dpi or ~15.8 dots/mm. WA seismograms are recorded at a rate of 1 mm/sec; thus, spatial aliasing of the scanned image occurs at frequencies above ~7.8 Hz. The trace-following algorithm, which produces the digitized record, does not reliably follow the scanned WA seismogram trace when large excursions at frequencies above ~2 Hz are present. In an attempt to circumvent these limitations, we tried photographically enlarging the original WA seismogram by 4×, but sufficient trace detail was lost in the enlargement process that we were again thwarted.

Inversion for BDSN δM_L and M_L

Between 18 September 1992 and 6 September 1995, more than 14,000 SWA seismograms were generated for the purpose of determining M_L from the maximum trace amplitudes. This data set was reduced to 9148 SWA records by requiring that the earthquake be located within the western United States, that the maximum trace amplitudes be at least 0.05 for both components at each BDSN station recording the earthquake, and that at least two BDSN stations recorded the earthquake (the resulting events are shown in Fig. 2). The last requirement is so that M_L estimates can be differenced to eliminate the need to simultaneously determine the M_L of each event along with the δM_L's for each BDSN station.

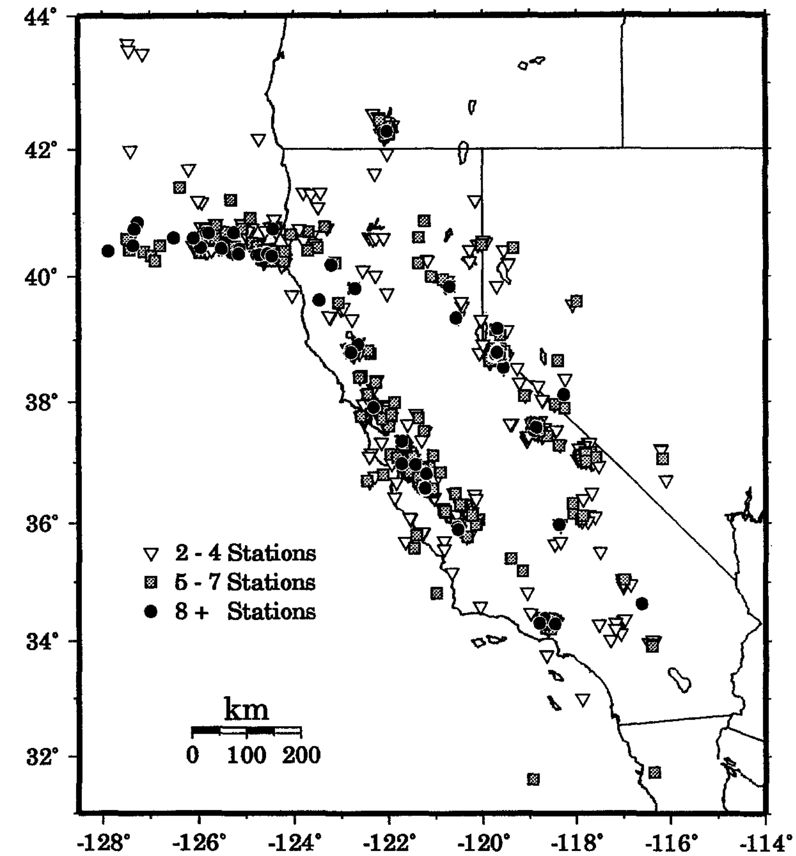

Figure 2. Map of California and vicinity showing the locations of the events used to determine the BDSN δM_L and $-\log A_0(\Delta)$. The different symbols indicate the number of BDSN stations that recorded the event. Inverted triangles, shaded squares, and solid circles represent 2 to 4, 5 to 7, and 8 + stations recording the event, respectively. Five events, either north of 44° latitude or east of $-114°$ longitude, were omitted from the plot.

We solved for the BDSN δM_L using two methods: an "absolute" method where we solved simultaneously for the M_L of each event and the δM_L for each station, and a "differential" method where we solved for only the δM_L for each station by differencing the equations to eliminate the need to solve for the M_L of each event. For both methods, we constrained the δM_L for ARC, BKS, MHC, and MIN to the values given in Table 2 so that the δM_L, and hence the M_L of the events, would not be biased. After the initial inversions were done, observations with absolute M_L residuals larger than 0.6 were culled, and the inversions were repeated. The results are given in Table 3 (for both solutions) and Appendix D (for the "absolute" solution). Note that the δM_L results for the two methods are not significantly different. Subsequently, we adopted the average δM_L of the two solutions (as given in Table 3) for the routine BDSN determination of M_L. The resulting M_L residual distribution is shown in Figure 5. Note that the standard error is 0.201 M_L units and that the residuals are approximately normally distributed. This standard error is essentially the same as the 0.203 standard error we obtained when determining M_L from the WA seismograms at the four original stations (ARC, BKS, MHC, and MIN) for events listed in Appendix A. The observation that the data variance does not change, when we switch from analog to digital determination of M_L, is also reassuring and an indication that the M_L estimation process is stationary.

Inversion for BDSN $-\log A_0(\Delta)$

In the process of analyzing the BDSN δM_L's presented above, we discovered that the M_L residual distribution contained significant systematic differences as a function of distance, as shown in Figure 6. This is not surprising since Richter's attenuation function $[-\log A_0(\Delta)]$ is relevant to southern California, and this study encompasses a much larger region. Biases in the $-\log A_0(\Delta)$ have been noted previously by Hutton and Boore (1987) for southern California and by Bakun and Joyner (1984) for central California, and they derived new attenuation functions for the two regions.

Since this study encompasses a much larger region, we decided to also invert for perturbations to $-\log A_0(\Delta)$. Several methods for parameterizing the perturbations to $-\log A_0(\Delta)$ were tried systematically, and it was determined that a cubic spline with knots at 0, 25, 75, 150, and 300 km best fit the observed M_L residual pattern. Subsequently, we inverted for perturbations to $-\log A_0(\Delta)$ with the additional imposed constraints that $-\log A_0$ (Δ = 100 km) = 3.0 (in agreement with Richter's definition) and that $d[-\log A_0(\Delta = 0 \text{ km})]/d\Delta = 0$ (to avoid large perturbations where there is little data). The results are shown in Figure 7 and Table 4. The largest perturbations to $-\log A_0(\Delta)$, approaching $+0.1$ in amplitude, occur at distances less than 30 km and again around 200 km, and they are due to crustal structural

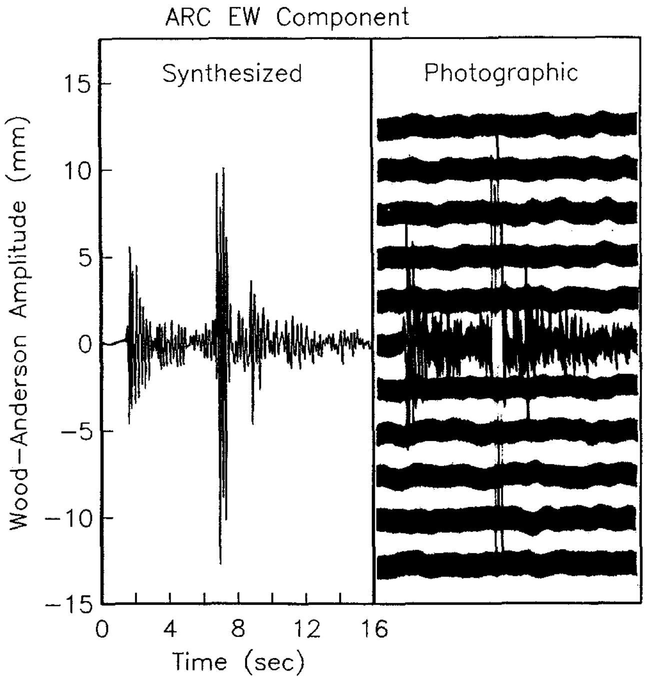

Figure 3. Comparison of the corresponding SWA and WA seismograms, recorded by the E–W component at ARC, for an M_L 3.0 earthquake that occurred 30 km southwest of ARC. Note that while the maximum trace amplitude registered on the two records differ by less than 2%, the waveforms differ considerably in their high-frequency detail. These seismograms were chosen as representative of the comparisons that have been done.

Table 3

δM_L for the New BDSN Stations

Station	δM_L* (abs)	δM_L† (diff)	δM_L‡ (avg)
CMB	+0.237 ± 0.0056	+0.243 ± 0.007	+0.240 ± 0.0090
HOPS	+0.329 ± 0.0185	+0.318 ± 0.026	+0.324 ± 0.0319
JRSC	+0.142 ± 0.0092	+0.131 ± 0.013	+0.139 ± 0.0159
KCC§			+0.39 ± 0.105
ORV	+0.413 ± 0.0067	+0.462 ± 0.009	+0.428 ± 0.0112
PKD1	−0.208 ± 0.0076	−0.174 ± 0.010	−0.198 ± 0.0126
SAO	+0.308 ± 0.0060	+0.327 ± 0.007	+0.314 ± 0.0092
STAN	−0.235 ± 0.0105	−0.229 ± 0.013	−0.233 ± 0.0167
WDC	+0.457 ± 0.0075	+0.516 ± 0.009	+0.484 ± 0.0117
YBH	+0.504 ± 0.0095	+0.488 ± 0.012	+0.499 ± 0.0153

*δM_L—δM_L derived from absolute inversion (including solving for M_L).
†δM_L—δM_L derived from differential inversion (without solving for M_L).
‡δM_L—adopted BDSN δM_L to be applied in determining BDSN M_L (average of δM_L* and δM_L†).
§δM_L derived from Table 7 data.

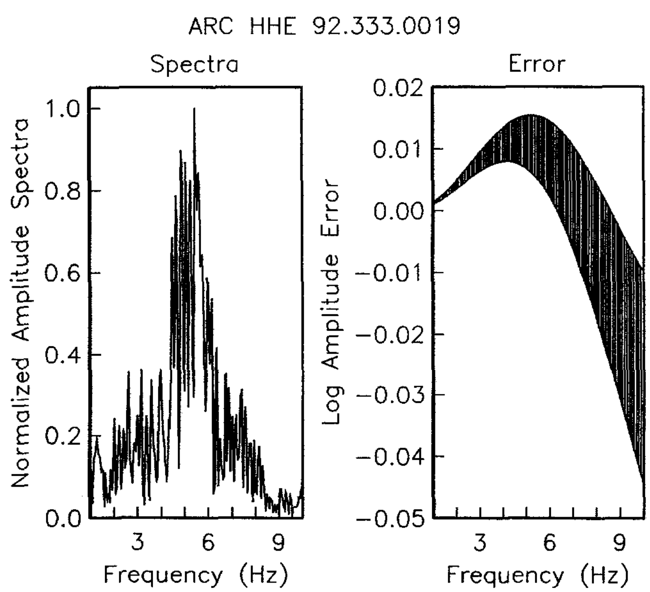

Figure 4. Amplitude spectrum for the SWA record shown in Figure 3 and estimates of the amplitude error range due to the discrete sampling (shaded range) and due to ignoring the FIR antialias filter response and the discrete sampling (curved shape of shaded region).

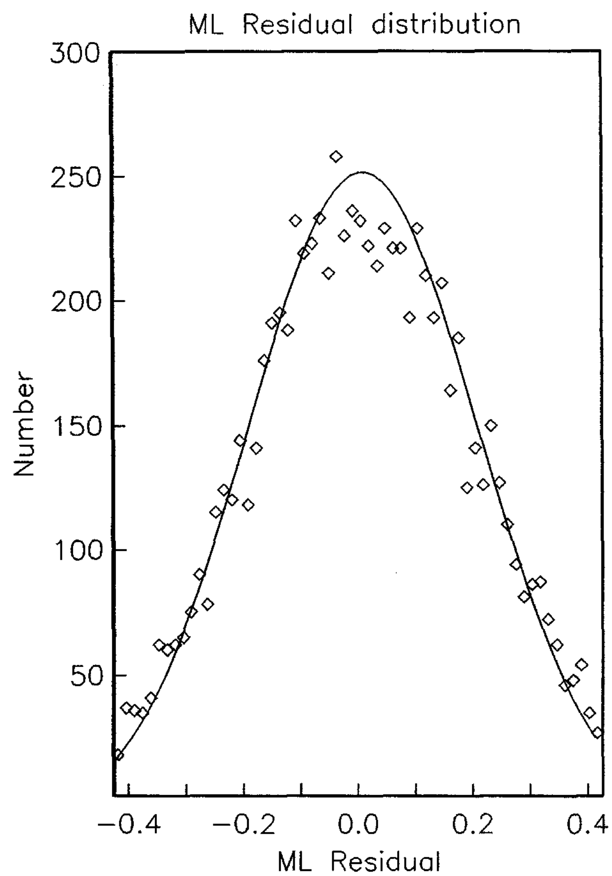

Figure 5. M_L residual histogram for the 9148 observations used in the inversion. The open diamonds are the number of observations, and the solid line is the least-squares fit normal distribution. The standard error of a single observation is 0.201 M_L units.

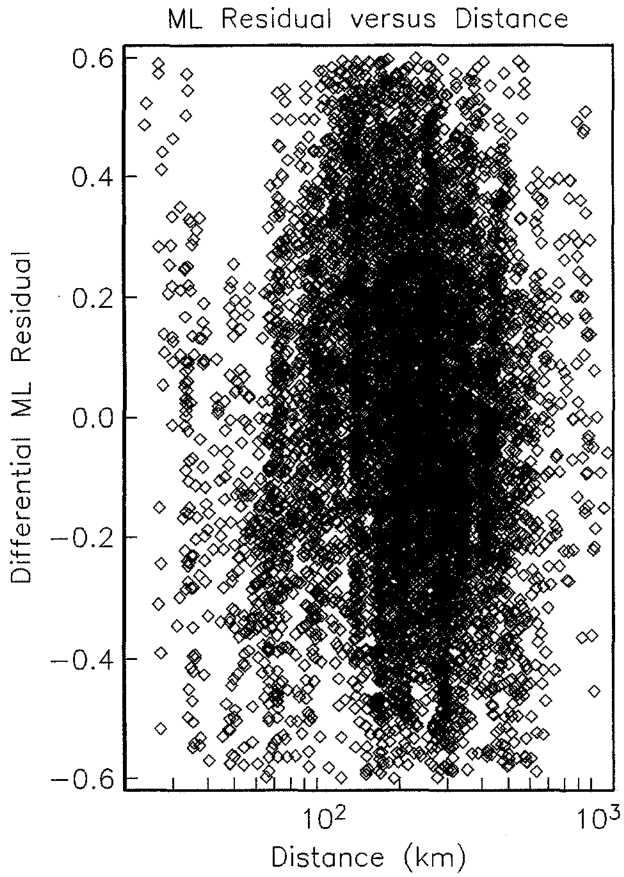

Figure 6. BDSN-derived M_L differential residual distribution versus distance. Note the significant structure in the scatter plot at distances less than 300 km, which implies that Richter's $-\log A_0(\Delta)$ is biased for the much larger geographical region considered in this study.

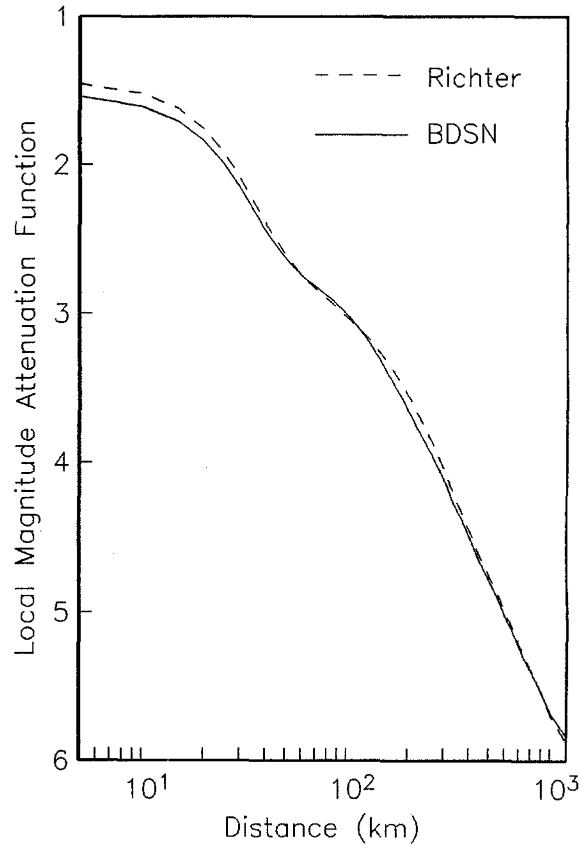

Figure 7. Comparison of $-\log A_0(\Delta)$ for BDSN and Richter. Note that the largest differences are at distances less than 30 km and around 200 km. These differences are due in part to the higher resolution of this study and to variations in the crustal structure between northern California (this study) and southern California (Richter). The embayment in both curves in the 20- to 120-km range is caused by the crustal structure where internally reflected waves produce an amplification of the seismic wave field.

differences between southern and northern California. Basically, the overall shape of $-\log A_0(\Delta)$ is due to geometrical spreading and attenuation of the seismic wave field and the embayment in the 20- to 120-km range is due to amplification of the seismic wave field caused by internal crustal reflections. Using the BDSN-derived $-\log A_0(\Delta)$ when determining M_L reduces the overall variance by 10%. However, in order to maintain continuity, we decided to employ Richter's $-\log A_0(\Delta)$, as given in Table 4, for routine BDSN determination of M_L.

Comparison with M_w and other M_L Estimates

A linear least-squares regression between the M_L determined here and the corresponding M_w determined from BDSN broadband waveform inversion (Pasyanos *et al.*, 1996) for 75 events ($3.6 \leqq M_L \leqq 6.8$), listed in Appendix E and plotted in Fig. 8, is

$$M_W = (0.997 \pm 0.020) \cdot M_L - (0.050 \pm 0.131). \quad (3)$$

Since the uncertainties in M_w and M_L, given in Appendix E, are of the same order, the regression was done bilinearly to minimize the normal distance between the sample points and the regression line. Within the uncertainties in the regression, $M_w \approx M_L$. Equation (3) is consistent with the results of Hanks and Kanamori (1979).

A comparison of M_L determined here with the corresponding M_L determined using TERRAscope stations (H. Kanamori, personal comm., 1995) is given in Table 5 for 10 recent earthquakes. The average difference between the two M_L estimates (TERRAscope − BDSN) is -0.084 ± 0.053, which is not significant. Thus, there is no evidence for a systematic bias between the two M_L estimates.

A comparison of M_L determined here with the corresponding M_L determined by University of Nevada, Reno (UNR) (Savage and Anderson, 1995), is given in Table 6 for 10 recent earthquakes. The average difference between the two M_L estimates (UNR − BDSN) is -0.42 ± 0.064, which

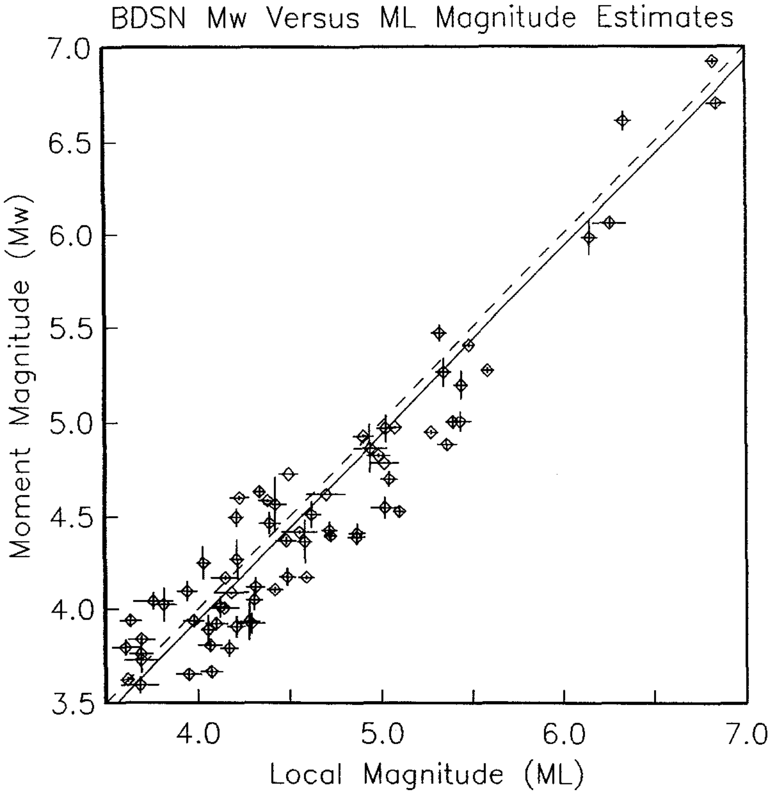

Figure 8. Comparison of M_L and M_w, both derived from the BDSN broadband data. A least-squares fit to the data (regressed on both axes because the uncertainties are of the same order) is given by the solid line. Note that the regression demonstrates that M_L and M_w are not significantly different over the $3.6 \leqq M_L \leqq 6.8$ range. A dashed line running through the origin with unity slope is given for comparison. The M_w data are the average of the M_w's determined by body waveform inversion and by surface waveform inversion (Pasyanos *et al.,* 1996). The data are given in Appendix E.

is quite significant. Thus, on average, the UNR-determined M_L are 0.4 smaller than the corresponding BDSN-determined M_L. This bias has been noted previously (Evernden, 1975), and the difference between magnitudes is not explained by average attenuation differences and is in need of further study (M. K. Savage, personal comm., 1996).

Prediction of δM_L

The wide range of the BDSN δM_L's from -0.2 at soft alluvial sites to $+0.5$ at hard-rock sites led to the question of whether or not δM_L could be reliably predicted from the site characteristics. The two most obvious site characteristics that could influence δM_L are the average rigidity (μ) of the rock and the average curvature (κ) of the local terrain in the vicinity of the station. Subsequently, we estimated the average μ of the bedrock lithology from geologic maps (Jennings, 1969) and the physical properties of rocks (Carmichael, 1989), as given in Table 1. We also estimated the average κ of the local terrain within a 500-m radius of the site by fitting a three-dimensional quadric surface through high-resolution digitized terrain data (Edwards and Batson, 1990) and determined the average κ at the site, as also given in Table 1. A least-squares regression of log μ and κ to the δM_L data (see Fig. 9) gives the following:

$$\delta M_L = (0.597 \pm 0.032)\cdot \log \mu + (0.025 \pm 0.018)\cdot \kappa, \quad (4)$$

where μ is in units of 10^{11} dynes/cm^2 and κ is in units of km^{-1}. The result is that δM_L for a station can basically be predicted from knowledge of the average μ of the site, and δM_L is relatively insensitive to average κ of the local terrain.

When we initially regressed δM_L against μ and κ, BKS and MHC were the largest outliers, both being more than $+0.2$. This was puzzling, and, subsequently, it was determined (David L. Jones, personal comm., 1995) that the surface rocks at both BKS and MHC (μ given in parenthesis in Table 1) are very thin (perhaps less than 200 m), and, at both sites, the subsurface rocks have a lower μ. At the dominant frequencies (~5 Hz, say) and corresponding wavelengths (~140 m, say) associated with maximum trace amplitudes (see Fig. 4), the surface rocks are basically transparent to the seismic wave field, and the δM_L is primarily influenced by μ of the subsurface rocks. Eaton (1992) also found that δM_L varies systematically with bedrock lithology. Thus the subsurface μ values, given in Table 1 for BKS and MHC, were adopted for all subsequent calculations.

As a test, we used data from the newest BDSN station at Kaiser Creek (KCC) (see Table 1) that became operational on 8 December 1995. KCC is sited in a 1000-ft tunnel excavated in solid granite in the Sierra Nevada with an estimated μ of $3.4\cdot 10^{11}$ dynes/cm^2 and, from equation (4), a predicted δM_L of $+0.36$. Subsequently, we extracted broadband KCC data for several recent earthquakes, as shown in Table 7. Comparing the KCC-determined M_L with the M_L determined from the rest of the BDSN stations, we see that $\delta M_L = +0.39 \pm 0.103$ for KCC, which is in agreement with the above prediction.

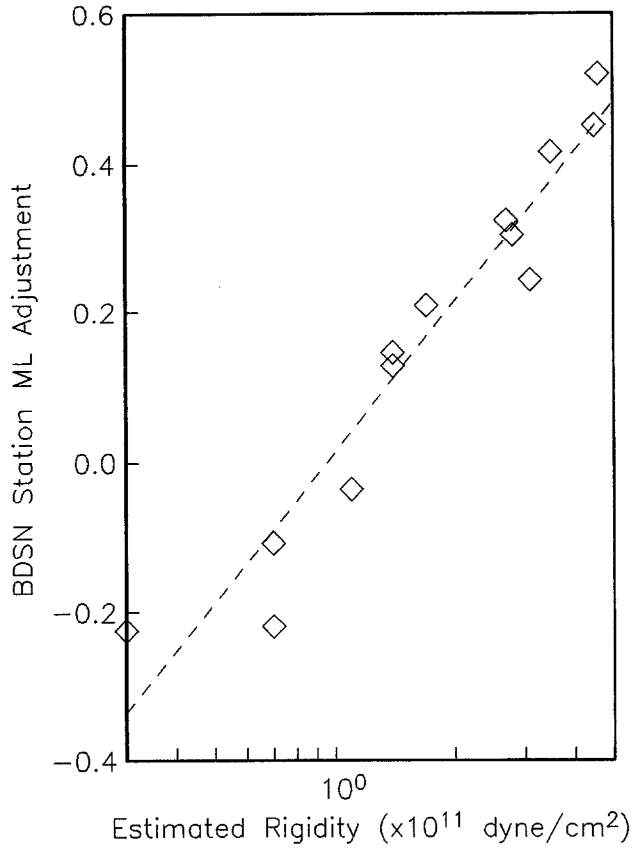

Figure 9. Comparison of the BDSN δM_L and the estimated average μ of the surrounding rock. The open diamonds are the BDSN station data, and the dashed line is the least-squares fit of the δM_L's and the estimated μ for each station. Note that the δM_L is approximately 0.6 * log (μ) (equation 4), so we can predict δM_L to within approximately ± 0.1 for a station if we have knowledge of the average μ of the surrounding rock to an accuracy of $\pm 50\%$.

Table 4
BDSN $-\log A_0(\Delta)$

Δ	$-\log A_0$*	$-\log A_0$†	Δ	$-\log A_0$*	$-\log A_0$†
0	1.4	1.489	260	3.8	3.933
5	1.4	1.489	270	3.9	3.976
10	1.5	1.588	280	3.9	4.020
15	1.6	1.685	290	4.0	4.063
20	1.7	1.782	300	4.0	4.107
25	1.9	1.976	310	4.1	4.151
30	2.1	2.168	320	4.1	4.195
35	2.3	2.359	330	4.2	4.240
40	2.4	2.448	340	4.2	4.278
45	2.5	2.537	350	4.3	4.311
50	2.6	2.625	360	4.3	4.344
55	2.7	2.713	370	4.3	4.378
60	2.8	2.744	380	4.4	4.412
65	2.8	2.776	390	4.4	4.446
70	2.8	2.809	400	4.5	4.480
80	2.9	2.870	410	4.5	4.515
85	2.9	2.901	420	4.5	4.549
90	3.0	2.934	430	4.6	4.584
95	3.0	2.969	440	4.6	4.619
100	3.0	3.000	450	4.6	4.649
110	3.1	3.064	460	4.6	4.674
120	3.1	3.132	470	4.7	4.699
130	3.2	3.203	480	4.7	4.725
140	3.2	3.272	490	4.7	4.750
150	3.3	3.341	500	4.7	4.775
160	3.3	3.407	510	4.8	4.800
170	3.4	3.470	520	4.8	4.826
180	3.4	3.530	530	4.8	4.851
190	3.5	3.589	540	4.8	4.877
200	3.5	3.645	550	4.8	4.902
210	3.6	3.699	560	4.9	4.927
220	3.65	3.751	570	4.9	4.952
230	3.7	3.798	580	4.9	4.978
240	3.7	3.844	590	4.9	5.003
250	3.8	3.889	600	4.9	5.028

*Richter's $-\log A_0(\Delta)$ (Δ in km) from Table 22-1 in Richter (1958).
†BDSN $-\log A_0(\Delta)$. For $\Delta \geqq 600$ km, use $-\log A_0(\Delta) = 2.9492 \cdot \log(\Delta) - 3.1753$.

Conclusions

We can successfully generate SWA seismograms, for the purpose of measuring the maximum trace amplitudes, using a basic convolution procedure that ignores the effects of the FIR antialias filter and the sampling error inherent in discrete sampling. We recommend that 80-samples/sec data be utilized when generating SWA seismograms. However, lower sampling rates can also be utilized without excessive loss of accuracy as long as the frequencies associated with the maximum trace amplitudes are below approximately 1/10 of the sampling rate.

We can indeed produce a seamless Berkeley M_L catalog when changing from WA to SWA seismogram measurement of the maximum trace amplitudes by utilizing the average BDSN δM_L's listed in Tables 2 and 3 and Richter's $-\log A_0(\Delta)$ given in Table 4. Utilizing the BDSN $-\log A_0(\Delta)$ (Table 4) reduces the variance by 10%. However, we decided to use Richter's $-\log A_0(\Delta)$ in order to maintain continuity in the Berkeley M_L catalog since the BDSN $-\log A_0(\Delta)$ is a potential source of bias when comparing the current BDSN SWA–derived M_L with the Berkeley M_L published over the past five decades.

A linear regression of M_w versus M_L determined using BDSN broadband records shows that M_w and M_L track each other over at least the $3.6 \leqq M_L \leqq 6.8$ range. A comparison between the BDSN- and TERRAscope-determined M_L indicates that they are not significantly different. A similar comparison between the BDSN-determined M_L and the corresponding UNR-determined M_L indicates a significant difference in that the UNR M_L is 0.42 $\pm$ 0.064 smaller. This difference in magnitude cannot be explained solely by differences in $-\log A_0(\Delta)$ between California and the western Great Basin.

The δM_L for a new BDSN station can be predicted within

Table 5
Comparison of BDSN and TERRAscope-Determined M_L

Date/Time	$M_L \pm \sigma$ (BDSN)	$M_L^* \pm \sigma$ (TERRA)	Diff†	M_w‡ (BDSN)	M_E‡ $\pm \sigma$ (TERRA)
93.042.1239	4.50 ± 0.062	4.26 ± 0.36	−0.24		4.23 ± 0.25
93.137.2320	6.26 ± 0.088	6.25 ± 0.21	−0.01	6.06	6.52 ± 0.21
93.140.2014	4.89 ± 0.042	4.60 ± 0.13	−0.29	4.60	4.52 ± 0.11
93.148.0447	5.02 ± 0.078	5.19 ± 0.18	+0.17	4.79	5.01 ± 0.10
94.079.2120	5.35 ± 0.040	5.37 ± 0.18	+0.02	5.26	5.35 ± 0.12
95.050.2124	4.68 ± 0.056	4.33 ± 0.23	−0.35		4.25 ± 0.17
95.064.0007	4.60 ± 0.043	4.66 ± 0.24	+0.06	4.17	4.40 ± 0.19
95.064.0248	4.43 ± 0.048	4.35 ± 0.24	−0.08	3.97	4.13 ± 0.21
95.127.1103	5.05 ± 0.046	4.99 ± 0.11	−0.06	4.66	4.92 ± 0.07
95.177.0840	5.22 ± 0.038	5.13 ± 0.21	−0.09	4.96	5.05 ± 0.14

*TERRAscope-determined M_L.

†M_L difference (TERRAscope − BDSN). The average difference is −0.084 ± 0.053.

‡BDSN M_w and TERRAscope M_E (Kanamori, 1993) for comparison.

Table 6
Comparison of BDSN- and UNR-Determined M_L

Date/Time	$M_L \pm \sigma$ (BDSN)	M_L (UNR)	Diff*	M_w (BDSN)	M_c† (UNR)
93.041.2148	5.03 ± 0.050	4.80	−0.23	4.55	4.59
93.062.1530	3.49 ± 0.093	2.93	−0.56		3.79
93.087.0734	3.91 ± 0.041	3.91	0.00		3.52
93.110.2116	3.35 ± 0.059	2.76	−0.59		3.48
93.119.1222	3.62 ± 0.062	3.03	−0.59		3.47
93.137.2320	6.26 ± 0.088	5.90	−0.36	6.06	6.1
93.137.2336	5.04 ± 0.055	4.37	−0.67		4.38
93.137.2342	4.36 ± 0.069	4.01	−0.35		3.48
93.140.0117	4.39 ± 0.061	3.88	−0.51	4.34	3.94
93.150.1521	4.10 ± 0.107	3.75	−0.35		4.27

*M_L difference (UNR − BDSN). The average difference is −0.42 ± 0.064.

†Coda duration magnitude (Lee *et al.*, 1972) given for comparison.

a tenth from the average μ of the rock (or alluvium) on which the station is sited. δM_L ranges from approximately −0.2 on the softest alluvial sites to approximately +0.5 on the hardest-rock sites.

Acknowledgments

We acknowledge use of the facilities of the Northern California Earthquake Data Center (NCEDC) and the Geophysical Computing Laboratory (GCL) in extracting and processing the data. All BDSN waveform and phase data used in this study is available on the NCEDC, and it can be accessed over the World-Wide-Web at URL http://quake.geo.berkeley.edu. We also acknowledge the staff of the Seismographic Station who did the routine analysis that made this article possible. Hiroo Kanamori provided δM_L's derived from TERRAscope broadband records. Doug Dreger and Mike Pasyanos provided their BDSN-derived M_w's for comparison. This is Seismographic Station Contribution Number 96-05.

References

Anderson, J. A. and H. O. Wood (1925). Description and theory of the torsion seismometer, *Bull. Seism. Soc. Am.* **15,** 1–72.

Bakun, W. H. and W. B. Joyner (1984). The ML Scale in Central California, *Bull. Seism. Soc. Am.* **74,** 1827–1843.

Bolt, B. A. and R. D. Miller (1975). *Catalogue of Earthquakes in Northern California and Adjoining Regions: 1 January 1910–31 December 1972, Seismographic Stations,* University of California Press, Berkeley, pp. iv + 567.

Bolt, B. A., J. E. Friday, and R. A. Uhrhammer (1988). A PC-based Broadband Digital Seismograph Network, *Geophys. J.* **93,** 565–573.

Boore, D. M. (1989). The Richter scale: its development and use for determining earthquake source parameters, *Tectonophysics* **166,** 1–72.

Carmichael, R. S. (1989). *CRC Practical Handbook of Physical Properties of Rocks and Minerals,* CRC Press, Boca Raton, pp. xiii + 741.

Eaton, J. P. (1992). Determination of amplitude and duration magnitudes and site residuals from short-period seismographs in northern California, *Bull. Seism. Soc. Am.* **82,** 533–579.

Edwards, K. and R. M. Batson (1990). Experimental Shaded Relief Maps of California, Misc. Investigations Series, Shaded Relief, Map I-1848, U.S. Geol. Survey.

Evernden, J. F. (1975). Magnitude determination at regional and near-regional distances in the United States, *Bull. Seism. Soc. Am.* **57,** 591–639.

Gutenberg, B. and C. F. Richter (1942). Earthquake magnitude, intensity, energy, and acceleration, *Bull. Seism. Soc. Am.* **32,** 163–192.

Hanks, T. C. and H. Kanamori (1979). A moment magnitude scale, *J. Geophys. Res.* **84,** 2348–2350.

Hutton, L. K. and D. M. Boore (1987). The M_L scale in southern California, *Bull. Seism. Soc. Am.* **77,** 2074–2094.

Jennings, C. W. (1969). Geologic Atlas of California, California Division of Mines and Geology.

Kanamori, H. (1993). Determination of earthquake energy release and M_L using TERRAscope, *Bull. Seism. Soc. Am.* **83,** 330–346.

Lee, W. H. K., R. Bennet, and K. Meagher (1972). *A Method of Estimating Magnitude of Local Earthquakes from Signal Duration, U.S. Geol. Surv. Open-File Rept.,* p. 28.

Pasyanos, M. E., D. S. Dreger, and B. Romanowicz (1996). Towards a real-time estimation of regional moment tensors, *Bull. Seism. Soc. Am.* **86,** 000–000.

Richter, C. F. (1935). An instrumental earthquake magnitude scale, *Bull. Seism. Soc. Am.* **25,** 1–32.

Richter, C. F. (1958). *Elementary Seismology,* W. H. Freeman and Co., San Francisco.

Romanowicz, B., L. Gee, and R. Uhrhammer (1992). Berkeley Digital Seismic Network: a broadband network for northern and central California, *IRIS Newsletter* **XI,** 1–5.

Romney, C. F. and J. E. Meeker (1949). *Bulletin of the Seismographic Stations, University of California* **18,** 1–89.

Savage, M. K. and J. G. Anderson (1995). A local-magnitude scale for the western Great Basin–Eastern Sierra Nevada from synthetic Wood–Anderson seismograms, *Bull. Seism. Soc. Am.* **85,** 1236–1243.

Uhrhammer, R. A. (1989). Seismographic Recording at Berkeley (1887–1987), 109–122, in *Observatory Seismology,* J. J. Litehiser (Editors), University of California Press, Berkeley, pp. vii + 379.

Uhrhammer, R. A. and E. R. Collins (1990). Synthesis of Wood–Anderson seismograms from broadband digital records, *Bull. Seism. Soc. Am.* **80,** 702–716.

Table 7
KCC δM_L

Date/Time	Δ (km)	Az (deg)	M_L* ± σ (BDSN)	M_L† ± σ (KCC)	δM_L‡
95.347.0545	195.7	259.3	3.99 ± 0.047	3.89 ± 0.162	+0.10
95.347.0619	195.5	259.9	3.53 ± 0.029	3.36 ± 0.159	+0.17
95.347.0625	194.9	259.7	4.05 ± 0.026	4.03 ± 0.130	+0.02
95.351.0520	349.4	299.3	3.17 ± 0.048	3.30 ± 0.086	−0.13
95.356.0900	160.7	351.1	5.24 ± 0.045	4.53 ± 0.050	+0.71
95.357.0539	155.6	349.9	5.16 ± 0.042	4.63 ± 0.070	+0.53
95.361.0810	141.2	320.1	2.70 ± 0.060	1.93 ± 0.090	+0.77
95.362.1828	158.0	349.2	5.48 ± 0.043	4.87 ± 0.015	+0.61
95.362.2005	156.5	349.7	3.10 ± 0.121	2.32 ± 0.011	+0.78
96.002.0626	157.9	349.5	4.13 ± 0.049	3.28 ± 0.074	+0.85
96.007.1433	227.7	139.7	5.34 ± 0.029	4.70 ± 0.063	+0.66
96.011.0258	167.2	228.9	3.08 ± 0.064	3.28 ± 0.056	−0.20
96.011.1706	146.0	230.0	3.21 ± 0.093	2.97 ± 0.113	+0.24

*M_L derived using all BDSN stations but KCC.
†M_L derived using only KCC.
‡δM_L (BDSN − KCC) to be added to M_L estimate from KCC (equation 1). The average KCC δM_L = +0.39 ± 0.103.

Appendix A
WA Data Used to Verify Historical δM_L

Date	Time	Lat	Long	M_L ± σ	ARC* N	ARC* E	BKS* N	BKS* E	MHC* N	MHC* E	MIN* N	MIN* E
84/01/23	05:40	36.39	−121.88	5.07 ± 0.073	0.90	1.10	104.00	82.00	64.00	66.30	2.50	3.10
84/02/16	11:14	39.93	−117.76	5.18 ± 0.072	2.00	1.40	3.10	3.80	6.40	3.50	7.90	5.60
84/02/28	15:16	40.36	−125.90	5.16 ± 0.122	34.60	40.00	2.40	2.80	1.20	1.10	30.30	30.70
84/03/01	17:45	37.07	−116.05	5.52 ± 0.061	0.70	0.90	4.10	4.30	11.00	6.00	2.00	3.60
84/04/28	22:48	37.62	−118.91	4.66 ± 0.100	0.30	0.30	3.10	3.30	6.00	2.70	9.00	3.90
84/05/31	13:04	37.10	−116.05	5.55 ± 0.047	0.60	0.60	5.00	4.00	10.00	7.40	4.50	4.00
84/07/25	15:30	37.27	−116.41	5.35 ± 0.078	0.50	0.70	2.10	2.40	7.40	11.80	2.60	2.40
84/08/04	21:45	40.26	−124.58	4.70 ± 0.078	44.40	40.80	2.10	1.90	1.10	0.80	19.00	21.70
84/09/10	07:47	40.41	−127.46	4.46 ± 0.077	0.70	0.90	0.50	0.50	0.30	0.30	1.10	0.80
84/09/10	23:52	40.36	−127.24	4.67 ± 0.086	1.40	1.60	0.80	1.20	0.80	0.50	1.70	1.20
84/09/11	11:23	40.49	−127.23	4.62 ± 0.095	1.20	1.30	0.80	0.80	0.80	0.50	1.40	1.30
84/09/20	18:30	40.38	−125.62	4.83 ± 0.133	17.60	28.20	1.20	1.60	0.50	0.60	16.70	21.20
84/09/20	19:04	40.43	−127.19	4.84 ± 0.049	3.60	4.90	0.80	0.90	0.70	0.70	2.80	3.10
84/11/23	18:08	37.46	−118.61	6.12 ± 0.060	12.40	12.00	65.00	72.00	104.60	91.40	60.50	82.20
84/11/23	19:12	37.42	−118.61	5.54 ± 0.046	1.70	1.50	16.50	16.00	46.60	61.90	16.90	18.80
84/11/26	16:21	37.45	−118.65	5.63 ± 0.043	3.40	1.90	27.50	20.00	71.20	71.30	15.10	17.40
85/01/07	06:17	40.40	−126.53	4.85 ± 0.107	8.50	5.90	1.50	1.30	0.70	0.35	5.50	10.40
85/01/24	11:27	38.16	−118.84	5.20 ± 0.069	1.00	0.90	23.30	22.80	26.40	13.10	7.30	14.20
85/03/06	01:52	38.95	−122.68	3.52 ± 0.077	0.30	0.50	4.60	3.70	0.60	0.50	0.90	1.30
85/03/23	18:30	37.18	−116.08	5.13 ± 0.069	0.30	0.40	2.00	1.60	4.80	3.00	1.10	0.90
85/04/18	16:29	39.11	−122.03	3.70 ± 0.088	0.60	0.70	2.80	1.80	0.80	0.50	4.40	8.10
85/05/12	13:55	40.39	−124.96	4.32 ± 0.096	6.90	8.90	0.80	0.80	0.35	0.35	9.40	6.00
85/05/28	07:56	39.51	−119.48	4.34 ± 0.034	0.30	0.30	1.75	2.25	2.20	2.00	7.40	7.80
85/12/05	15:00	37.05	−116.04	5.34 ± 0.074	0.60	0.40	2.90	2.10	8.00	6.10	1.50	1.80
86/02/11	01:15	41.72	−125.25	4.92 ± 0.048	47.40	38.50	1.40	0.95	0.70	0.55	6.40	8.50

(*continued*)

Appendix A (*Continued*)

Date	Time	Lat	Long	$M_L \pm \sigma$	ARC* N	ARC* E	BKS* N	BKS* E	MHC* N	MHC* E	MIN* N	MIN* E
86/05/31	08:47	36.63	−121.27	4.65 ± 0.052	0.30	0.30	33.80	22.60	45.40	57.30	1.40	1.50
86/06/25	20:27	37.27	−116.50	5.39 ± 0.043	0.70	0.70	3.80	3.60	9.60	4.40	3.10	3.10
86/10/12	06:43	38.72	−123.50	3.96 ± 0.081	2.10	1.10	6.30	5.90	1.80	1.10	0.80	1.60
86/10/16	19:25	37.22	−116.46	5.40 ± 0.062	0.60	0.90	5.30	4.20	9.70	4.00	2.80	2.20
86/11/14	16:00	37.10	−116.05	5.55 ± 0.047	0.60	1.00	5.30	4.50	9.00	6.70	3.80	2.80
87/02/14	07:26	36.15	−120.33	5.29 ± 0.086	0.80	1.10	22.00	19.50	51.30	33.40	12.30	11.80
87/04/16	04:52	40.44	−124.41	4.17 ± 0.105	20.60	41.90	0.30	0.40	0.30	0.30	5.90	7.00
87/04/30	13:30	37.23	−116.42	5.36 ± 0.038	0.60	0.60	3.50	3.00	7.40	5.40	2.40	3.50
87/05/01	22:22	39.81	−123.17	3.78 ± 0.094	5.90	4.30	0.70	0.50	0.40	0.30	4.30	4.80
87/07/28	18:55	38.38	−118.17	4.60 ± 0.046	0.40	0.30	2.60	2.10	2.10	1.60	1.70	2.50
87/08/13	14:00	37.08	−115.93	5.60 ± 0.061	1.00	1.40	4.50	4.30	12.50	4.80	2.90	3.40
87/10/01	14:42	34.06	−118.08	6.07 ± 0.044	1.90	2.20	10.50	12.00	15.90	15.30	8.10	12.60
87/10/04	10:59	34.07	−118.10	5.58 ± 0.045	0.80	0.60	4.40	3.60	8.10	3.70	2.80	3.10
87/10/23	16:00	37.14	−116.08	5.17 ± 0.045	0.40	0.50	1.40	1.30	3.60	3.10	1.40	1.60
88/02/15	18:10	37.31	−116.47	5.28 ± 0.079	1.10	1.00	2.20	2.90	5.00	3.70	1.50	1.80
88/02/20	08:39	36.80	−121.30	5.09 ± 0.064	1.00	0.80	103.50	82.30	130.60	100.10	8.00	9.00
88/07/16	05:23	39.17	−123.30	3.64 ± 0.043	0.90	0.80	1.60	1.20	1.00	0.70	1.10	1.50
88/07/26	03:26	36.56	−121.18	4.59 ± 0.048	0.40	0.60	14.70	11.20	30.50	21.60	1.50	1.70
88/08/30	18:00	37.09	−116.07	5.09 ± 0.079	0.60	0.50	0.90	0.80	3.40	2.00	1.20	1.10
88/09/30	00:30	41.63	−121.55	4.27 ± 0.035	3.00	2.20	0.40	0.40	0.50	0.30	14.10	14.00
88/10/13	14:00	37.09	−116.03	5.65 ± 0.053	1.10	1.10	5.70	5.20	15.00	6.80	4.30	3.50
88/10/20	17:33	38.80	−122.80	3.66 ± 0.120	0.70	0.70	8.80	5.30	1.30	1.00	0.60	0.50
88/10/25	14:43	38.71	−123.44	3.82 ± 0.067	0.70	0.60	7.10	5.00	1.50	1.20	0.70	1.10
89/01/19	06:53	33.92	−118.63	5.27 ± 0.019	0.35	0.30	2.40	2.40	3.80	2.90	1.40	1.10
89/05/04	03:37	40.57	−127.54	4.63 ± 0.075	1.10	1.30	0.60	0.80	0.40	0.35	1.50	1.40
89/06/22	21:15	37.28	−116.41	5.29 ± 0.043	0.35	0.55	2.80	2.80	6.90	4.40	2.75	2.80
89/08/08	23:15	39.48	−122.93	4.08 ± 0.135	7.40	7.70	1.60	1.50	0.80	0.65	10.55	16.20
89/12/08	15:00	37.23	−116.41	5.26 ± 0.052	0.40	0.45	2.80	2.50	6.70	4.70	1.65	2.80
90/01/06	05:35	40.45	−125.67	4.30 ± 0.054	6.10	5.00	0.70	0.40	0.30	0.30	2.40	2.50
90/01/27	22:06	38.79	−122.74	3.52 ± 0.160	0.30	0.35	13.00	9.30	0.75	0.60	0.40	0.35
90/02/28	23:43	34.14	−117.70	6.21 ± 0.039	2.55	2.00	14.80	11.00	27.40	28.00	11.80	14.50
90/04/03	21:12	38.84	−122.79	3.63 ± 0.147	0.70	0.65	9.00	9.00	0.80	1.00	0.40	0.50
90/04/18	15:46	36.95	−121.70	5.06 ± 0.087	2.35	1.50	123.00	141.00	156.00	132.00	6.90	8.00
90/04/28	04:47	37.87	−122.01	4.22 ± 0.084	0.40	0.70	135.70	148.60	45.00	39.00	2.00	3.20
90/06/13	16:00	37.26	−116.42	5.63 ± 0.047	1.10	1.50	5.60	7.10	14.80	9.10	4.80	4.50
90/07/31	03:19	42.42	−126.68	5.06 ± 0.082	6.00	7.10	1.30	1.00	1.00	1.20	1.60	1.40
90/09/26	04:14	40.45	−125.80	4.66 ± 0.123	14.50	16.00	0.80	0.80	0.40	0.30	10.00	10.00
90/10/03	12:57	40.50	−126.98	4.37 ± 0.105	1.50	1.10	0.40	0.40	0.60	0.70	0.50	0.40
90/10/12	17:30	37.25	−116.49	5.54 ± 0.061	2.00	1.30	4.00	3.60	10.50	6.00	4.00	5.00
90/10/24	06:15	38.05	−119.15	5.82 ± 0.050	7.20	7.60	68.70	58.50	67.00	97.00	71.00	86.00
90/12/07	21:51	40.67	−125.33	4.51 ± 0.076	7.60	17.40	0.80	0.70	0.70	0.50	6.90	5.00
91/03/24	03:42	36.96	−121.74	4.55 ± 0.059	0.50	0.30	39.60	33.10	67.50	66.50	2.50	3.00
91/04/04	19:00	37.30	−116.31	5.31 ± 0.089	0.40	0.30	4.10	3.00	10.50	6.50	1.80	2.00
91/04/16	15:30	37.24	−116.44	5.39 ± 0.074	0.40	0.60	3.70	3.90	13.00	7.50	2.50	3.00
91/07/13	06:09	41.89	−125.87	4.79 ± 0.062	5.90	9.00	0.80	0.70	0.60	0.60	3.40	5.50
91/09/17	21:10	35.83	−121.32	5.14 ± 0.053	0.80	1.10	36.00	27.10	50.00	41.20	1.70	2.80
92/07/05	21:18	34.58	−116.32	5.72 ± 0.039	0.80	1.20	3.50	2.80	5.60	4.60	3.10	2.80

*WA maximum trace amplitude (A) in mm.
The standard error is 0.203 M_L units.

Appendix B

Calibration Parameters for the WA Seismographs

Station	Component*	V_S†	T_S† (sec)	h_S†	Instrument‡
ARC	S–N	2080	0.81	0.75	LG
	E–W	1920	0.81	0.66	LG
BKS	S–N	2060	0.80	0.66	LG
	W–E	2110	0.80	0.71	LG
MHC	S–N	2010	0.80	0.70	H
	E–W	2030	0.77	0.71	H
MIN	N–S	2010	0.80	0.69	H
	E–W	2190	0.79	0.74	H

*Component is given in terms of up–down on the WA seismogram.

†V_S = static magnification, T_S = free period, and h_S = fraction of critical damping of standard Wood–Anderson torsion seismograph.

‡Manufacturer; H = Henson and LG = Lehner and Griffith.

The above calibration parameters were determined within the last year of operation of the instruments. The scatter around the adopted values of $V_S = 2080$, $T_S = 0.8$, and $h_S = 0.7$ is typical. Note that the average $V_S = 2050 \pm 30$, which is not significantly different than the adopted V_S value of 2080 ± 60. For details about the WA calibration procedure, see Appendix A in Uhrhammer and Collins (1990).

Appendix C

SWA and WA Maximum Trace Amplitude Comparison

Date	Time	Lat.	Lon.	Stn	Diff*
91/09/11	01:30	37.00	−121.94	MHC	+0.064
91/09/19	09:07	36.88	−121.66	MHC	+0.042
91/09/19	09:07	36.88	−121.66	BKS	−0.083
91/09/21	14:31	37.48	−121.81	MHC	+0.024
91/10/07	12:11	37.53	−121.39	MHC	+0.064
91/12/14	08:12	37.40	−121.75	MHC	−0.067
92/01/21	03:56	37.42	−121.70	MHC	−0.086
92/02/15	14:36	37.69	−121.59	BKS	−0.081
92/04/23	04:50	33.96	−116.32	MHC	+0.067
92/04/23	23:10	37.36	−121.69	MHC	+0.072
92/04/26	07:41	40.45	−124.63	MHC	+0.035
92/10/20	05:28	35.92	−120.49	MHC	+0.015
92/10/31	17:00	36.80	−121.54	MHC	+0.081
92/11/23	20:59	38.08	−121.86	BKS	+0.048
92/11/27	16:00	34.34	−116.90	MHC	−0.058
92/12/26	22:11	43.93	−127.89	ARC	−0.017
93/05/18	23:48	37.06	−117.86	MIN	−0.031
93/05/19	14:13	37.13	−117.78	MIN	+0.017

*M_L difference (SWA − WA).

Note that the average M_L difference ($+0.005 \pm 0.014$) is not significant, which implies that the WA- and SWA-determined maximum trace amplitudes are, on average, the same. The observed 0.0035 variance of the M_L differences is consistent with the variance due to the scatter in the V_S of the individual WA seismographs (see Appendix B) and due to the errors caused by the FIR filter and discrete sampling (see Fig. 4). Therefore, we adopt the WA δM_L from this study (given in Table 2) to determine M_L from the SWA maximum trace amplitudes.

Appendix D

$M_L \geq 3.8$ Events Used in This Study

Date	Time	Lat	Lon	M_L	σ	No. Obs.	Date	Time	Lat	Lon	M_L	σ	No. Obs.	Date	Time	Lat	Lon	M_L	σ	No. Obs.
92/09/18	17:00	37.21	−116.21	4.47	0.094	06	92/11/25	02:40	35.05	−117.03	4.25	0.041	04	92/11/26	21:41	34.98	−117.01	4.24	0.078	06
92/11/27	16:00	34.34	−117.01	6.19	0.119	08	92/11/27	18:32	34.36	−116.98	4.36	0.063	06	92/11/27	20:02	40.39	−127.13	4.87	0.078	10
93/01/16	06:29	37.03	−121.49	5.45	0.064	06	93/01/18	23:27	38.86	−122.78	4.24	0.148	04	93/02/10	21:48	40.40	−119.56	5.03	0.075	08
93/02/11	12:39	35.03	−117.03	4.50	0.062	06	93/03/19	18:23	34.91	−117.01	3.80	0.053	04	93/03/20	06:56	34.01	−117.29	3.98	0.053	08
93/03/25	13:34	45.04	−122.66	5.73	0.092	06	93/03/28	07:34	40.44	−119.35	3.91	0.053	12	93/04/04	05:21	35.95	−120.53	4.40	0.061	12
93/04/19	02:30	40.59	−127.48	4.14	0.083	10	93/04/29	08:21	35.60	−112.27	5.79	0.048	14	93/05/17	08:45	39.59	−118.00	4.03	0.059	10
93/05/17	23:20	37.16	−117.69	6.26	0.088	10	93/05/17	23:36	37.14	−117.82	5.04	0.074	08	93/05/17	23:42	37.08	−117.81	4.36	0.073	06
93/05/17	23:51	37.12	−117.73	4.49	0.113	06	93/05/18	00:00	37.15	−117.81	3.97	0.082	06	93/05/18	00:18	37.15	−117.84	3.92	0.095	06
93/05/18	00:56	37.01	−117.80	3.82	0.102	08	93/05/18	01:03	37.07	−117.58	5.40	0.076	10	93/05/18	05:10	37.12	−117.90	3.88	0.058	10
93/05/18	08:19	37.08	−117.92	3.86	0.075	08	93/05/18	10:28	37.05	−117.90	3.90	0.064	14	93/05/18	10:56	36.97	−117.69	4.02	0.101	08
93/05/19	03:17	37.10	−117.90	3.92	0.073	10	93/05/19	03:20	37.15	−117.83	4.94	0.052	14	93/05/19	14:13	37.13	−117.80	5.37	0.054	14
93/05/20	01:17	37.18	−117.80	4.39	0.104	08	93/05/20	09:19	36.10	−117.72	3.82	0.061	06	93/05/20	20:14	36.10	−117.72	4.89	0.042	06
93/05/26	19:11	37.07	−117.80	4.09	0.109	08	93/05/26	20:35	37.01	−117.91	3.84	0.067	06	93/05/28	04:47	35.18	−119.15	5.02	0.078	10
93/05/30	15:21	36.70	−116.11	4.10	0.107	08	93/05/31	08:55	34.12	−117.06	4.24	0.064	08	93/06/03	02:23	37.12	−117.89	3.88	0.081	08
93/06/08	19:59	37.03	−117.82	4.31	0.119	06	93/06/19	00:52	40.69	−124.36	3.88	0.114	04	93/06/22	14:50	37.15	−117.76	3.84	0.089	06
93/07/06	02:13	38.57	−119.56	4.04	0.040	18	93/07/08	18:27	34.95	−116.85	3.90	0.043	06	93/07/08	22:57	34.30	−117.17	3.83	0.044	04
93/07/21	00:23	36.10	−117.62	4.09	0.066	08	93/07/27	21:17	40.29	−124.64	4.12	0.062	12	93/08/08	11:44	37.01	−117.80	4.19	0.065	14
93/08/11	05:48	37.52	−118.91	4.74	0.051	16	93/08/11	22:33	37.30	−121.70	4.95	0.088	10	93/08/22	18:08	36.49	−117.68	3.83	0.022	04
93/09/06	10:32	35.97	−118.38	4.11	0.062	16	93/09/21	03:16	42.23	−122.08	4.54	0.102	08	93/09/21	04:16	42.22	−122.08	4.53	0.049	10
93/09/21	04:34	42.27	−122.07	4.30	0.067	10	93/09/21	06:14	42.26	−122.11	4.91	0.055	18	93/09/21	07:28	42.32	−122.12	3.84	0.104	08
93/09/22	07:01	37.20	−116.20	4.24	0.042	06	93/09/23	06:21	41.93	−122.03	4.24	0.054	08	93/09/24	16:53	42.31	−122.02	3.98	0.071	06
93/09/25	02:26	37.43	−118.62	3.88	0.066	10	93/10/11	07:19	36.56	−121.23	4.22	0.039	18	93/10/18	21:49	31.60	−118.94	4.88	0.033	10
93/10/18	22:47	40.44	−125.37	3.80	0.064	12	93/10/19	04:47	37.52	−118.90	3.95	0.061	14	93/10/21	14:37	36.15	−118.08	4.30	0.077	12
93/10/22	16:30	36.06	−117.96	3.97	0.042	08	93/10/23	18:45	40.61	−126.51	5.33	0.057	22	93/10/26	09:24	35.03	−116.96	3.89	0.061	10
93/10/29	11:53	38.11	−118.27	4.11	0.042	16	93/11/06	00:29	37.57	−118.87	3.86	0.047	12	93/11/14	12:25	35.93	−120.55	4.99	0.063	16
93/11/23	19:32	40.32	−126.96	4.01	0.109	10	93/11/26	02:08	40.24	−126.90	4.05	0.044	14	93/12/04	22:15	42.27	−122.03	5.49	0.033	16
93/12/04	23:23	42.30	−122.07	3.94	0.047	10	93/12/04	23:50	42.36	−121.91	3.96	0.060	08	93/12/08	09:06	35.01	−116.99	4.05	0.112	04
93/12/10	00:27	37.09	−117.82	3.92	0.042	08	93/12/16	00:43	38.55	−119.56	3.98	0.059	18	93/12/31	18:08	42.24	−121.98	3.87	0.075	10
93/12/31	21:29	37.61	−118.93	3.88	0.052	18	94/01/07	09:39	42.28	−122.00	3.97	0.064	10	94/01/09	19:03	42.33	−122.01	4.07	0.061	10
94/01/11	10:53	36.98	−121.72	4.32	0.051	18	94/01/17	12:30	34.21	−118.59	6.85	0.054	10	94/01/17	13:06	34.25	−118.60	4.62	0.052	08
94/01/17	13:26	34.32	−118.50	4.70	0.046	10	94/01/17	13:44	34.35	−118.59	4.13	0.036	08	94/01/17	13:56	34.28	−118.67	4.87	0.042	12
94/01/17	14:14	34.33	−118.49	4.49	0.059	12	94/01/17	14:46	38.82	−122.43	4.06	0.057	10	94/01/17	14:50	34.32	−118.50	4.00	0.051	06
94/01/17	15:07	34.30	−118.52	4.27	0.052	10	94/01/17	15:14	34.35	−118.50	3.92	0.059	04	94/01/17	15:45	34.37	−118.65	4.12	0.046	08
94/01/17	15:54	34.37	−118.67	4.98	0.051	12	94/01/17	17:56	34.23	−118.63	4.62	0.051	10	94/01/17	18:51	34.34	−118.48	3.93	0.040	08
94/01/17	19:35	34.31	−118.50	4.08	0.061	06	94/01/17	19:43	34.37	−118.68	4.49	0.053	10	94/01/17	20:02	34.40	−118.60	3.95	0.038	08
94/01/17	20:05	34.34	−118.57	4.10	0.035	08	94/01/17	20:46	34.30	−118.63	5.40	0.035	12	94/01/17	22:19	34.35	−118.68	4.20	0.080	06
94/01/17	22:31	34.32	−118.50	4.31	0.036	08	94/01/17	22:57	34.35	−118.66	3.91	0.047	04	94/01/17	23:49	34.35	−118.70	4.38	0.054	08
94/01/18	00:39	34.38	−118.61	4.37	0.050	10	94/01/18	00:43	34.38	−118.76	5.57	0.067	08	94/01/18	04:01	34.36	−118.66	4.80	0.048	08
94/01/18	04:31	34.36	−118.49	4.02	0.036	08	94/01/18	05:19	34.34	−118.72	4.03	0.038	10	94/01/18	07:23	34.33	−118.67	4.37	0.044	12
94/01/18	11:35	34.22	−118.66	4.30	0.034	12	94/01/18	13:24	34.31	−118.61	4.57	0.045	10	94/01/18	15:19	34.22	−118.63	3.94	0.027	08
94/01/18	15:23	34.38	−118.60	5.06	0.029	10	94/01/18	16:23	34.37	−118.62	4.10	0.040	08	94/01/19	04:40	34.36	−118.62	4.58	0.050	10
94/01/19	09:13	34.31	−118.77	4.14	0.041	08	94/01/19	14:09	34.20	−118.56	4.46	0.044	12	94/01/19	14:46	34.30	−118.52	3.95	0.073	08
94/01/19	21:11	34.38	−118.69	5.60	0.035	16	94/01/19	22:27	42.34	−122.02	4.25	0.048	12	94/01/20	05:58	34.38	−118.74	4.01	0.034	08
94/01/20	06:58	34.36	−118.74	4.04	0.055	08	94/01/20	15:42	40.52	−124.86	4.57	0.068	14	94/01/21	18:39	34.30	−118.52	4.69	0.059	08

Appendix D (*Continued*)

Date	Time	Lat	Lon	M_L	σ	No. Obs.	Date	Time	Lat	Lon	M_L	σ	No. Obs.	Date	Time	Lat	Lon	M_L	σ	No. Obs.
94/01/21	18:42	34.31	−118.51	4.26	0.043	06 :	94/01/21	18:53	34.30	−118.49	4.58	0.058	08 :	94/01/23	08:55	34.30	−118.47	4.32	0.048	08
94/01/24	04:15	34.34	−118.60	4.81	0.040	10 :	94/01/24	05:50	34.36	−118.67	4.46	0.057	08 :	94/01/24	05:54	34.36	−118.66	4.50	0.066	08
94/01/27	17:19	34.27	−118.61	4.42	0.056	10 :	94/01/28	20:09	34.37	−118.53	4.39	0.033	08 :	94/01/29	12:16	34.28	−118.66	4.45	0.051	10
94/02/01	08:01	37.27	−118.37	4.28	0.059	12 :	94/02/02	11:24	34.29	−118.66	3.89	0.037	10 :	94/02/03	09:05	42.75	−110.72	6.18	0.072	12
94/02/03	16:23	34.30	−118.48	4.34	0.052	08 :	94/02/04	02:42	42.71	−110.88	5.43	0.054	06 :	94/02/05	08:51	34.41	−118.72	3.89	0.048	06
94/02/06	13:19	34.29	−118.52	4.05	0.050	06 :	94/02/21	13:40	40.43	−125.14	4.22	0.043	18 :	94/02/25	12:59	34.36	−118.53	3.96	0.055	10
94/03/02	10:21	40.66	−125.42	3.96	0.095	12 :	94/03/07	16:49	38.84	−119.70	4.00	0.055	14 :	94/03/13	16:59	40.36	−125.16	4.43	0.035	18
94/03/20	21:20	34.28	−118.52	5.35	0.040	12 :	94/03/23	02:59	31.72	−116.36	5.27	0.038	10 :	94/03/31	20:00	36.18	−120.32	4.38	0.063	14
94/03/31	20:02	36.16	−120.31	4.12	0.059	12 :	94/04/06	19:01	34.19	−117.18	5.10	0.022	06 :	94/04/08	17:53	34.47	−118.99	3.98	0.035	08
94/04/21	16:37	36.30	−120.45	4.56	0.097	12 :	94/04/24	19:06	36.51	−121.06	3.83	0.049	12 :	94/05/04	04:09	34.33	−118.49	3.91	0.037	08
94/05/09	14:14	41.98	−127.42	4.16	0.150	04 :	94/05/19	16:45	36.57	−121.25	3.95	0.054	16 :	94/05/25	12:56	34.31	−118.43	4.73	0.026	08
94/05/30	03:22	36.03	−117.90	3.98	0.049	06 :	94/06/02	03:27	34.27	−118.50	3.84	0.046	08 :	94/06/15	05:59	34.31	−118.43	4.24	0.024	08
94/06/19	10:39	40.36	−124.60	4.91	0.055	16 :	94/06/26	08:42	37.91	−122.32	4.15	0.074	18 :	94/06/29	06:10	40.49	−127.36	4.24	0.064	18
94/07/11	06:50	34.27	−118.75	3.81	0.030	06 :	94/07/13	17:52	43.45	−127.15	4.43	0.034	04 :	94/08/01	21:34	34.63	−116.62	4.88	0.045	16
94/08/07	15:10	33.99	−116.36	4.00	0.034	08 :	94/08/09	12:47	40.34	−124.77	3.98	0.042	16 :	94/08/28	01:22	36.81	−121.20	4.06	0.037	18
94/09/01	15:15	40.45	−125.95	6.83	0.038	22 :	94/09/01	15:56	40.50	−125.49	4.10	0.105	06 :	94/09/01	16:25	40.46	−125.57	4.32	0.068	08
94/09/01	17:14	40.38	−125.85	3.80	0.140	06 :	94/09/07	19:10	37.51	−121.26	4.15	0.080	14 :	94/09/08	09:49	40.80	−125.62	3.89	0.133	12
94/09/08	09:52	40.85	−127.26	4.23	0.070	16 :	94/09/08	11:19	40.73	−127.31	3.83	0.053	06 :	94/09/08	12:19	40.75	−127.33	4.04	0.060	16
94/09/12	12:23	38.83	−119.68	6.16	0.043	20 :	94/09/12	12:57	38.75	−119.69	3.82	0.071	08 :	94/09/12	23:57	38.82	−119.66	5.45	0.040	20
94/09/13	07:33	38.74	−119.53	3.88	0.088	08 :	94/09/13	11:49	38.77	−119.65	4.21	0.049	16 :	94/09/13	21:22	38.82	−119.66	4.49	0.046	18
94/09/14	06:16	38.77	−119.65	3.90	0.057	14 :	94/09/15	00:45	38.78	−119.69	3.97	0.064	14 :	94/09/15	07:54	38.80	−119.54	4.04	0.047	14
94/09/17	02:59	38.74	−119.70	4.05	0.047	08 :	94/09/17	12:36	38.73	−119.71	4.18	0.049	20 :	94/09/19	07:25	38.75	−119.60	4.07	0.066	10
94/09/19	14:06	38.73	−119.75	4.08	0.059	16 :	94/09/20	03:17	38.75	−119.61	4.19	0.084	04 :	94/09/20	03:37	38.76	−119.62	4.13	0.041	16
94/09/20	03:45	38.75	−119.62	3.96	0.048	12 :	94/09/20	15:38	38.76	−119.60	4.91	0.037	20 :	94/09/20	15:40	38.74	−119.60	4.99	0.059	18
94/09/20	15:46	38.74	−119.62	3.86	0.108	06 :	94/09/21	02:09	40.44	−124.67	4.70	0.106	08 :	94/09/21	06:51	38.77	−119.68	3.84	0.058	12
94/09/21	08:58	38.73	−119.73	3.85	0.060	14 :	94/09/21	18:47	38.77	−119.62	4.02	0.050	12 :	94/09/25	22:30	38.76	−119.62	3.82	0.064	16
94/10/06	00:15	38.75	−119.73	3.93	0.126	04 :	94/10/10	03:07	38.75	−119.64	4.87	0.049	18 :	94/10/14	00:57	40.34	−124.72	4.25	0.043	20
94/10/19	00:49	35.51	−117.51	4.22	0.099	08 :	94/10/27	17:45	43.60	−127.46	5.32	0.115	08 :	94/10/28	09:32	43.50	−127.44	4.34	0.100	08
94/11/13	21:13	40.48	−126.80	3.84	0.055	12 :	94/11/14	01:28	40.36	−124.55	4.39	0.050	18 :	94/11/17	20:29	42.44	−122.19	4.49	0.053	10
94/11/18	20:50	39.17	−119.69	4.48	0.053	16 :	94/11/20	04:31	34.01	−116.40	4.17	0.035	08 :	94/12/04	00:38	40.21	−123.13	3.95	0.085	12
94/12/06	03:36	34.30	−118.43	4.00	0.030	08 :	94/12/06	03:48	34.29	−118.47	5.04	0.043	16 :	94/12/07	03:21	37.35	−121.71	3.82	0.068	16
94/12/16	03:03	40.69	−125.25	4.44	0.073	20 :	94/12/20	10:27	35.89	−120.53	5.08	0.041	20 :	94/12/20	22:14	38.73	−119.72	4.03	0.043	16
94/12/21	05:50	38.74	−119.70	4.31	0.045	18 :	94/12/25	07:59	36.11	−117.87	3.98	0.041	12 :	94/12/26	14:10	40.75	−124.43	5.32	0.044	20
95/01/06	00:12	38.78	−119.71	4.72	0.044	18 :	95/01/08	01:00	40.42	−127.43	4.50	0.050	10 :	95/01/11	13:53	40.33	−124.68	4.33	0.057	10
95/01/29	03:12	47.39	−122.40	4.98	0.043	18 :	95/02/01	22:04	40.87	−121.24	3.96	0.073	12 :	95/02/08	02:13	40.78	−123.35	4.21	0.102	12
95/02/08	09:36	40.76	−124.39	4.35	0.121	12 :	95/02/12	17:53	37.95	−118.46	3.82	0.035	10 :	95/02/18	20:17	38.79	−119.71	4.33	0.047	18
95/02/19	04:03	40.60	−126.09	6.34	0.045	22 :	95/02/19	21:24	33.96	−116.47	4.68	0.056	08 :	95/02/27	09:54	40.69	−125.82	3.84	0.041	16
95/02/28	19:40	40.40	−127.88	4.47	0.055	22 :	95/02/28	23:09	38.92	−122.64	4.03	0.036	20 :	95/03/01	10:55	40.68	−125.77	4.34	0.032	22
95/03/05	00:07	37.59	−118.86	4.60	0.043	20 :	95/03/05	02:48	37.58	−118.86	4.43	0.048	20 :	95/04/04	05:08	34.27	−117.53	3.81	0.048	08
95/04/22	14:31	38.76	−119.72	4.59	0.040	22 :	95/04/23	08:41	36.58	−121.25	5.03	0.046	20 :	95/05/07	11:03	33.90	−116.40	5.05	0.046	12
95/05/08	18:19	38.66	−118.40	3.81	0.052	10 :	95/05/15	21:57	40.44	−125.51	4.19	0.093	18 :	95/05/17	02:29	39.81	−122.71	4.43	0.060	20
95/05/27	05:49	38.80	−119.69	4.11	0.060	20 :	95/06/12	21:23	36.32	−118.09	3.97	0.103	10 :	95/06/16	04:20	36.75	−121.37	3.98	0.055	14
95/06/18	22:23	39.84	−120.71	4.42	0.046	18 :	95/06/21	21:17	33.00	−117.88	4.13	0.024	06 :	95/06/26	08:40	34.30	−118.79	5.28	0.038	22
95/07/05	12:36	38.79	−119.69	3.93	0.037	16 :	95/07/12	21:58	36.57	−121.23	4.13	0.045	16 :	95/07/31	12:34	37.05	−116.17	4.34	0.076	10

The standard error is 0.203 M_L units.

Appendix E
BDSN M_w and M_L Comparison

Date/Time	Lat	Long	$M_w \pm \sigma$	$M_L \pm \sigma$	Location
93.016.0629	37.03	−121.46	5.01 ± 0.050	5.45 ± 0.064	Gilroy
93.041.2148	40.40	−119.58	4.55 ± 0.058	5.03 ± 0.075	Pyramid Lake
93.094.0521	35.95	−120.51	4.47 ± 0.059	4.40 ± 0.061	Parkfield
93.137.2320	37.16	−117.69	6.06 ± 0.021	6.26 + 0.088	Eureka Valley
93.139.1413	37.13	−117.78	4.89 ± 0.024	5.37 ± 0.054	Eureka Valley
93.148.0447	35.18	−119.11	4.79 ± 0.000	5.02 ± 0.079	Bakersfield
93.223.2233	37.30	−121.69	4.87 ± 0.126	4.94 ± 0.089	San Felipe
93.262.2049	38.12	−122.45	3.47 ± 0.020	3.47 ± 0.073	Rogers Creek
93.262.2110	38.12	−122.44	3.58 ± 0.014	3.45 ± 0.101	Rogers Creek
93.266.0621	41.93	−122.03	4.60 ± 0.010	4.23 ± 0.053	Klamath Falls
93.284.0719	36.56	−121.22	4.27 ± 0.107	4.21 ± 0.038	Pinnacles
93.294.1437	36.15	−118.03	3.92 ± 0.055	4.29 ± 0.075	Owens Valley
93.318.1225	35.93	−120.52	4.83 ± 0.010	4.99 ± 0.063	Parkfield
93.338.2215	42.27	−122.03	5.41 ± 0.010	5.49 ± 0.032	Klamath Falls
94.011.1053	36.98	−121.72	4.12 ± 0.051	4.31 ± 0.051	Watsonville
94.017.1230	34.21	−118.54	6.71 ± 0.022	6.85 ± 0.054	Northridge
94.017.1756	34.22	−118.58	4.51 ± 0.070	4.62 ± 0.051	Northridge
94.017.2046	34.30	−118.58	5.01 ± 0.031	5.39 ± 0.035	Northridge
94.019.2111	34.38	−118.62	5.27 ± 0.014	5.59 ± 0.033	Northridge
94.032.0801	37.27	−118.36	3.93 ± 0.101	4.28 ± 0.059	Bishop
94.052.1340	40.43	−125.10	4.50 ± 0.049	4.21 ± 0.042	Mendocino
94.079.2120	34.28	−118.47	5.27 ± 0.075	5.34 ± 0.041	Northridge
94.096.1901	34.19	−117.10	4.53 ± 0.025	5.10 ± 0.022	San Bernadino
94.111.1637	36.30	−120.44	4.42 ± 0.009	4.55 ± 0.096	Coalinga
94.139.1643	36.57	−121.24	4.09 ± 0.054	3.21 ± 0.051	Pinnacles
94.139.1645	36.57	−121.24	4.09 ± 0.054	3.94 ± 0.053	Pinnacles
94.144.2011	40.92	−124.90	3.60 ± 0.043	3.69 ± 0.101	Mendocino
94.145.1256	34.31	−118.39	4.40 ± 0.030	4.72 ± 0.026	Northridge
94.170.1039	40.36	−124.58	4.93 ± 0.008	4.91 ± 0.054	Petrolia
94.177.0842	37.91	−122.32	4.17 ± 0.011	4.15 ± 0.074	Berkeley
94.183.1343	40.24	−124.47	3.94 ± 0.024	3.64 ± 0.058	Mendocino
94.184.2342	37.89	−118.26	3.62 ± 0.012	3.62 ± 0.026	Bishop
94.213.2134	34.63	−116.52	4.41 ± 0.053	4.87 ± 0.044	Landers
94.240.0122	36.81	−121.19	3.89 ± 0.079	4.06 ± 0.037	Tres Pinos
94.241.0509	38.81	−122.82	4.02 ± 0.090	3.26 ± 0.059	Geysers
94.244.1515	40.44	−125.90	6.93 ± 0.015	6.83 ± 0.037	Mendocino
94.250.1910	37.51	−121.26	4.01 ± 0.011	4.14 ± 0.080	Modesto
94.255.1223	38.83	−119.67	5.98 ± 0.093	6.15 ± 0.043	Double Spring Flat
94.255.2357	38.82	−119.66	5.20 ± 0.074	5.44 ± 0.039	Double Spring Flat
94.256.1149	38.76	−119.65	3.91 ± 0.057	4.21 ± 0.048	Double Spring Flat
94.256.2122	38.82	−119.66	4.18 ± 0.049	4.49 ± 0.046	Double Spring Flat
94.260.0259	38.74	−119.71	3.48 ± 0.055	4.05 ± 0.047	Double Spring Flat
94.260.1236	38.73	−119.71	3.79 ± 0.045	4.17 ± 0.048	Double Spring Flat
94.262.0725	38.75	−119.61	3.81 ± 0.023	4.07 ± 0.065	Double Spring Flat
94.262.1406	38.73	−119.74	3.67 ± 0.029	4.07 ± 0.058	Double Spring Flat
94.264.0209	40.44	−124.66	4.62 ± 0.000	4.70 ± 0.106	Mendocino FZ
94.270.1125	40.65	−124.06	3.84 ± 0.015	3.70 ± 0.074	Eureka
94.283.0307	38.75	−119.64	4.39 ± 0.039	4.86 ± 0.048	Double Spring Flat
94.284.2313	36.85	−121.61	3.73 ± 0.067	3.69 ± 0.088	San Juan Bautista
94.318.0128	40.36	−124.51	4.59 ± 0.007	4.38 ± 0.049	Mendocino

(continued)

Appendix E (*Continued*)

Date/Time	Lat	Long	$M_w \pm \sigma$	$M_L \pm \sigma$	Location
94.321.2029	42.44	−122.18	4.37 ± 0.019	4.48 ± 0.055	Klamath
94.338.1035	37.35	−121.71	3.76 ± 0.089	3.69 ± 0.063	Alum Rock
94.341.0321	37.35	−121.71	4.02 ± 0.091	3.82 ± 0.068	Alum Rock
94.354.1027	35.89	−120.50	4.97 ± 0.004	5.08 ± 0.040	Parkfield
94.355.0550	38.74	−119.70	4.05 ± 0.057	4.31 ± 0.044	Double Spring Flat
94.360.1410	40.76	−124.37	5.47 ± 0.045	5.32 ± 0.043	Eureka
95.006.0012	38.78	−119.71	4.43 ± 0.045	4.72 ± 0.043	Double Spring Flat
95.008.0100	40.42	−127.39	4.73 ± 0.001	4.50 ± 0.051	Petrolia
95.032.2204	40.87	−121.24	3.65 ± 0.028	3.95 ± 0.071	Burney
95.050.0403	40.60	−126.03	6.61 ± 0.050	6.34 ± 0.044	Gorda Plate
95.059.2309	38.92	−122.63	4.25 ± 0.090	4.03 ± 0.039	Clear Lake
95.060.1055	40.68	−125.71	4.64 ± 0.026	4.34 ± 0.032	Offshore Petrolia
95.064.0007	37.60	−118.84	4.17 ± 0.008	4.59 ± 0.042	Mammoth
95.112.1431	38.76	−119.71	4.37 ± 0.117	4.58 ± 0.040	Markleeville
95.113.0841	36.58	−121.24	4.97 ± 0.071	5.03 ± 0.045	Pinnacles
95.122.1256	40.18	−123.19	4.04 ± 0.045	3.76 ± 0.106	Covelo
95.126.1246	40.40	−123.70	3.79 ± 0.043	3.61 ± 0.073	Petrolia
95.127.1103	33.90	−116.28	4.70 ± 0.040	5.04 ± 0.046	Indio
95.135.2157	40.44	−125.49	4.09 ± 0.005	4.18 ± 0.092	Mendocino FZ
95.137.0229	39.81	−122.70	4.57 ± 0.148	4.42 ± 0.060	Covelo
95.147.0549	38.80	−119.69	3.92 ± 0.026	4.10 ± 0.059	Markleeville
95.167.0420	36.75	−121.37	3.94 ± 0.033	3.98 ± 0.054	Hollister
95.169.2223	39.84	−120.72	4.11 ± 0.016	4.42 ± 0.044	Quincy
95.177.0840	34.30	−118.70	4.95 ± 0.010	5.28 ± 0.037	Castaic
95.193.2158	36.57	−121.23	4.01 ± 0.057	4.12 ± 0.045	San Benito

Seismographic Station
475 McCone Hall
University of California
Berkeley, California 94720-4760

Manuscript received 24 January 1996.